Article (refereed) - postprint

1   **Assessing contributions of agricultural and non-agricultural emissions to**

2   **atmospheric ammonia in a Chinese megacity**

3   *Yunhua Chang*,[†, a] *Zhong Zou*, [‡, a] *Yanlin Zhang*,[†, *] *Congrui Deng*,[‡, *] *Jianlin Hu*,[△] *Zhihao*

4   *Shi*,[△] *Anthony J. Dore*, [‖] *and Jeffrey L. Collett Jr.*[‡]

5   [†]Yale-NUIST Center on Atmospheric Environment, Nanjing University of Information

6   Science & Technology, Nanjing 210044, China

7   [‡]Department of Environmental Science & Engineering, Institute of Atmospheric

8   Sciences, Fudan University, Shanghai 200433, China

9   [△]School of Environmental Science and Engineering, Nanjing University of Information

10   Science & Technology, Nanjing 210044, China

11   [‖]Centre for Ecology & Hydrology Edinburgh, Bush Estate, Penicuik, Midlothian EH26

12   0QB, UK

13   ⸸Department of Atmospheric Science, Colorado State University, Fort Collins,

14   Colorado, 80523 USA

15   ᵃEqually contributing co-authors

16

17

18

19   ABSTRACT Ammonia (NH_3) is the predominant alkaline gas in the atmosphere

20   contributing to formation of fine particles - a leading environmental cause of increased

21   morbidity and mortality worldwide. Prior findings suggest that NH_3 in the urban

22   atmosphere derives from a complex mixture of agricultural (mainly livestock production

23   and fertilizer application) and non-agricultural (e.g., urban waste, fossil fuel-related

24   emissions) sources; however, a citywide holistic assessment is hitherto lacking. Here

25   we show that NH_3 from non-agricultural sources rivals agricultural NH_3 source

26   contributions in the Shanghai urban atmosphere. We base our conclusion on four

27   independent approaches: (i) a full-year operation of a passive NH_3 monitoring network

2

28   at 14 locations covering urban, suburban, and rural landscapes; (ii) model-

29   measurement comparison of hourly NH_3 concentrations at a pair of urban and rural

30   supersites; (iii) source-specific NH_3 measurements from emission sources; and (iv)

31   localized isotopic signatures of NH_3 sources integrated in a Bayesian isotope mixing

32   model to make isotope-based source apportionment estimates of ambient NH_3. Results

33   indicate that non-agricultural sources and agricultural sources are both important

34   contributors to NH_3 in the urban atmosphere. These findings highlight opportunities to

35   limit NH_3 emissions from non-agricultural sources to help curb $PM_{2.5}$ pollution in urban

36   China.

37   **1 Introduction**

38   Atmospheric ammonia (NH_3) is the predominant alkaline gas in the atmosphere and

39   actively involved in atmospheric chemistry. In reactions with sulphuric acid and nitric

40   acid, formed via the oxidation of SO_2 and NO_x, respectively, NH_3 contributes to the

41   formation of NH_4^+ salts, which typically make up from 20 to 80% of atmospheric

42   particulate matter with an aerodynamic diameter less than 2.5 micrometers ($PM_{2.5}$).[1-5]

43   This fine particle formation has led to huge health and economic costs.[6-10]

44   There is an increasing importance of NH_3 emissions relative to SO_2 and NO_x

45   worldwide due to relatively slow reduction of NH_3 emissons.[11-17] Over 90% of NH_3

46   emissions in China, the United States and many European countries result from

47   agriculture, mainly including livestock production and NH_3-based fertilizer application;[6,]

48   [13, 15, 18-22] thus, agricultural NH_3 emissions are often blamed for high levels of

49   ammonium-containing $PM_{2.5}$.[1, 6, 7, 23, 24] However, in urban areas where agricultural

50   activities are mostly absent, a growing body of evidence suggests that non-agricultural

51   activities like wastewater treatment,[25] coal combustion,[26] solid garbage,[27] vehicular

52   exhaust,[28] and urban green space[29] also contribute to NH_3 emissions.[30] For example,

53   large vehicular NH_3 emissions from noble metal-based three-way catalysts (TWCs)

54   have been detected in chassis dynamometer vehicle experiments, road tunnel tests,

55   and ambient air measurements dating back to the 1980s.[31-42] Nevertheless, Yao et al.[43]

56   and Teng et al.[29] suggest that vehicular NH_3 emissions can be neglected and proposed

57   urban green spaces as the dominant contributor to urban atmospheric NH_3 in North

58   America and Northern China. There remains a long-standing and on-going controversy

59   regarding the relative contribution of agricultural and non-agricultural NH_3 emissions in

60   the urban atmosphere.[44-46]

61   In China, while there have been no long-term and nationwide NH_3 monitoring studies

62   like   the   U.S.   passive   Ammonia   Monitoring   Network   (AMoN,

63   http://nadp.sws.uiuc.edu/amon) affiliated with the National Atmospheric Deposition

64   Program (NADP),[47-49] numerous researchers have measured NH_4^+ concentrations in wet

65   deposition (i.e., precipitation) for more than 30 years.[50, 51] The data show that the annual

66   flux of NH_4^+ in wet deposition in China has increased in conjunction with the growth in

67   animal production and fertilizer application.[17, 50, 52, 53] Further, China's recent economic

68   boom has been coupled with accelerated urbanization.[54, 55] In 1978 less than 20% of

69   Chinese residents lived in cities. The population of its cities has quintupled over the past

70   40 years, reaching 813 million or nearly 60% of the total population.[56] At present, there

71   are three super-regions or city clusters in China: the Pearl River Delta (PRD), next to

72   Hong Kong; the Yangtze River Delta (YRD), which surrounds Shanghai; and Jing-jin-ji

73   (J^3), centered on Beijing.[57] In particular, the YRD region is arguably the most concentrated

74   set of adjacent urban conurbations in the world.[58] Huge cities place huge demands on

75   resource consumption and associated non-agricultural NH_3 emissions.[44] For example,

76   the region has continuously experienced double-digit growth in auto sales since 2009.[36]

77   The expanding motor vehicle population in its cities, in turn, is reshaping the urban

78   atmospheric composition.[59, 60] Meanwhile, the vast rural areas of the YRD region are

79   dominated by fluvial plains with fertile soil, and abundant production of rice and tea.[22]

80   According to Huang et al.,[22] livestock production, N-fertilizer application, and non-

81   agricultural sources (including sewage treatment, waste landfills, and human discharge)

82   in the YRD region in 2007 comprise 48%, 40%, and 12% of the total 459 kt NH_3 emissions,

83   respectively. The interplay of agricultural and non-agricultural NH_3 emissions in the region

84   provides an ideal study area to investigate their impact on ambient NH_3 concentrations

85   over time.

86   Taking Shanghai as an example, the present study aims to systematically elucidate

87   the role of non-agricultural NH_3 emissions contributing to ambient NH_3 in the urban

88   atmosphere through (1) investigating the spatial and temporal variability of NH_3

89   concentrations across various land use categories, (2) interpreting the consistency or

90   discrepancy of NH_3 concentrations between field measurements and chemical transport

91   model simulations, and (3) using stable isotopes as a tool to quantify source category

92   contributions to ambient NH_3 concentrations in the rural and urban atmospheres.

93   **2 Materials and methods**

94   **2.1 Site description**

95   The Yangtze River Delta or YRD region encompasses the nation's largest population

96   center, Shanghai, and major agricultural fields in eastern China. In order to obtain

97   information regarding the spatial and temporal variability of NH_3 concentrations in

98   Shanghai, we established a regional monitoring network of fourteen sites covering

99   urban (FD, HK, YP, HP, PT, JA, LW, XH, and PD), suburban (ZJ and CJ), and rural

100   (DH, SY and CM) landscapes (Fig. 1). Of particular importance are PD and DH, which

101   also serve as supersites intended to represent urban and rural settings, respectively. In

102   Shanghai, all ten state-control stations (SCS) of China's Ministry of Environmental

103   Protection were utilized. The advantages of selecting these SCS sites include (i) their

104   deliberate locations away from point and local sources of pollution, such as

105   transportation corridors, agricultural fields, livestock operations, and industrial

106   emissions; (ii) they have well-trained staff with long-term employment to sustain

107   continuous measurements; and (iii) they are equipped with refrigerators so that the

108   collected samples can be quickly stored to prevent potential contamination or sample

109   degradation. More detailed site descriptions can be found elsewhere.[36, 61] The

110   meteorology in Shanghai is typical of a subtropical monsoon system with four distinct

111   seasons. A summary of the average meteorological conditions can be found in SI Fig.

112   S1.

113   **2.2 Field sampling**

114   In order to obtain the spatial distributions of NH_3 concentrations over the Shanghai

115   region, from May 2014 to June 2015, weekly Ogawa PSDs (passive sampling devices,

116   Ogawa, FL, USA) were deployed at each site (from March 2017 to March 2018 for CM

117   and SY sites) under the protection of an opaque shelter for collecting ambient NH_3.

118   Between June and August of 2014, two Ogawa PSDs were deployed for monthly

119   collection at the urban PD site and the rural DH site for N isotopic analysis of NH_3. The

120   Ogawa PSD consists of a solid cylindrical polymeric body (2 cm diameter, 3 cm long)

121   housing a citric acid-coated glass fiber disk at each end as a duplicate to trap NH_3.[48] All

122   PSD components (including filters) were purchased from Ogawa USA, and sampling

123   procedures provided by the manufacturer (http://www.ogawausa.com) were strictly

124   followed throughout the campaign. After exposure, the filters were transferred with

125   tweezers into plastic vials (15 mL) and stored at -18 °C immediately. The samples were

126   delivered to the analytical laboratory monthly. The average relative percent difference

127   between duplicate Ogawa PSD samples was 5.5%.

128   In order to relate temporal variations of NH_3 concentrations to potential NH_3 sources,

129   the PD (urban) and DH (rural) sites were equipped with a Monitor for AeRosols and

130   Gases (MARGA, Applikon B.V., NL), allowing continuous characterization of the

131   inorganic components of $PM_{2.5}$ (NH_4^+, NO_3^-, SO_4^{2-}, Cl^-, Na^+, K^+, Ca^{2+}, Mg^{2+}) and water-

132   soluble gases (NH_3, SO_2, HCl, HONO and HNO_3) at hourly resolution.[62] This effort

133   builds upon our earlier effort[36] to look at the influence of on-road traffic on ambient NH_3

134   variability with different meteorology at the PD site. Details of the MARGA instrument

135   and its performance can be found elsewhere.[36] To complement the information obtained

136   from the MARGA monitoring campaign, additional measurements of tailpipe-emitted

137   NH_3 from 19 different vehicles equipped with three-way catalytic converters were carried

138   out in Nanjing, a megacity in the western Yangtze River Delta region, during April 2016,

139   following a method described elsewhere[63] and briefly summarized in SI Text S1.

140   **2.3 Laboratory analysis**

141   NH_4^+ concentrations in the H_2SO_4 absorbing solutions were measured using a

142   Dionex^{TM} ICS-5000$^+$ system (Thermo Fisher Scientific, Sunnyvale, USA) at the clean

143   laboratory (class 1000) of Yale-NUIST Center on Atmospheric Environment. The IC

144   system was equipped with an automated sampler (AS-DV). NH_4^+ in solutions was

145   measured using an IonPac CG12A guard column and CS12A separation column with

146   an aqueous methanesulfonic acid (MSA, 30 mM L^{-1}) eluent at a flow rate of 1 mL min^{-1}.

147   For the Ogawa passive samples, each filter pad was soaked in 8 mL deionized water

148   (18 MΩ·cm) in a 15 mL vial for 30 min with occasional shaking. Concentrations of NH_4^+

149   in extracts were analyzed using an ion chromatography system (883 Basic IC plus,

150   Metrohm Co., Switzerland) equipped with a Metrosep C4/4.0 cation column. The eluent

151   was 1.0 mmol L^{-1} HNO$_3$ + 1.0 mmol L^{-1} 2,6-pyridine dicarboxylic acid. The detection limit

152   for NH_4^+ was 2.8 μg L^{-1}, corresponding to an ambient NH_3 concentration of 0.1 ppb for a

153   seven-day sample.

154   For isotopic analysis, a robust and quantitative chemical method was used to

155   determine δ^{15}N-NH$_4^+$ based on the isotopic analysis of nitrous oxide (N_2O),[64] as detailed

156   and successfully applied in our previous studies.[61, 65] One of the advantages of this

157   method is that it is more suitable for low volume samples including those with low

158   nitrogen concentration. The standard deviation of δ^{15}N measurements determined from

159   the replicates is less than 0.3‰.

160   **2.4 Ammonia modeling**

161   The Community Multiscale Air Quality (CMAQ, v5.0.1) chemical transport model was

162   used to simulate hourly NH_3 and NH_4^+ concentrations in Shanghai with a 12 × 12 km^2

163   grid resolution.[66] Meteorological inputs were generated with the Weather Research and

164   Forecasting (WRF v3.6.1) model and the National Centers for Environmental Prediction

165   FNL Operational Model Global Tropospheric Analyses. The tropospheric analyses

166   dataset was used to provide initial and boundary conditions. A multi-resolution emission

167   inventory for China developed by Tsinghua University (http://www.meicmodel.org) was

168   used to define monthly anthropogenic emissions from China. Anthropogenic emissions

169   in 2012 including NH_3, SO_2, NO_x, volatile organic compounds, and PM were re-gridded

170   to the model grids. Open biomass burning emissions were generated from the Fire

171   INventory from NCAR, which is based on satellite observations.[66] Dust and sea salt

172   emissions were generated online during the CMAQ simulations. Biogenic emissions

173   were generated using the Model for Emissions of Gases and Aerosols from Nature

174   (v2.1). [66] The model configurations of CMAQ and WRF are similar to those utilized in a

175   previous nationwide study.[66]

176   **2.5 Bayesian mixing model**

177   Isotopic mixing models allow us to estimate the proportional contributions of multiple

178   sources (emission sources of NH_3 in this study) within a mixture (the ambient NH_3 in this

179   study).[67] By explicitly reflecting the uncertainties associated with multiple sources,

180   isotope fractionation, and isotopic signatures, the application of Bayesian methods to

181   stable isotope mixing models is able to generate robust probability estimates of source

182   proportions, being more appropriate in natural systems than simple linear mixing

183   models.[68, 69] Here a novel Bayesian methodology for analyzing mixing models

184   implemented in the software package SIAR (Stable Isotope Analysis in R)[70] was used to

185   resolve multiple NH_3 source categories by generating potential solutions of source

186   apportionment as true probability distributions. The generation of such source

187   contribution probability distributions is helpful in estimating likely ranges of source

188   contributions when the system solution is under-constrained (i.e., the number of sources

189   exceeds the number of different isotope system tracers + 1). The SIAR package is

190   available to download from the packages section of the Comprehensive R Archive

191   Network site (CRAN) - http://cran.r-project.org/, and has been widely applied in a

192   number of fields.[71-75] Model frame and computing methods are detailed in SI Text S2.

193   A comprehensive pool of isotopic source signatures of NH_3 (IS_NH_3) has been

194   established in our previous work[65] with the exception of "NH_3 slip from coal-fired power

195   plant".[76] These IS_NH_3 are typically found to lie between -50‰ and -10‰, with

196   occasional overlap between signatures from different source types.[65, 77] The NH_3

197   emissions were defined by four distinct source categories (Table 1): livestock breeding

198   (-29.1 ± 1.7‰), N-fertilizer application (-50.0 ± 1.8‰; urea application), combustion-

199   related sources (-14.0 ± 2.7‰; on-road traffic, NH_3 slip from coal-fired power plants),

200   and urban waste volatilized sources (-37.8 ± 3.6‰; wastewater treatment, municipal

201   solid waste, and human excreta).

202   **2.6 Ancillary information**

203   Hourly meteorological parameters (MSO Weather Sensor, MetOne Instruments, USA;

204   including wind direction, wind speed, relative humidity or RH, and temperature or *T*) in

205   Shanghai were provided by the Shanghai Meteorological Bureau. Bivariate polar plots

206   (BPP) were used to demonstrate how NH_3 concentrations vary with wind direction and

207   wind speed in polar coordinates, an effective diagnostic technique for discriminating

208   different source regions.[78-81] For creating BBPs, the open-source software "openair" in

209   R was used.[79]

210   **3 Results and discussion**

211   **3.1 Spatially-revolved sampling reveals urban areas as a hot spot of atmospheric NH_3**

212   A total of 702 duplicate passive samples were collected in this study. The passive

213   sampling sites are divided into three types: urban (461 samples), suburban (108

214   samples), and rural (133 samples), based on local land use and economic activities.

215   Weekly variations of atmospheric NH_3 concentrations at each observation site, and

216   annual and seasonal average NH_3 concentrations (mean ± 1 σ) among different sites

217   and site categories are plotted in Fig. 2 and Fig. 3, respectively. The observations from

218   the Ogawa passive samplers are mainly used to illustrate spatial distributions rather

219   than temporal variations of NH_3, due to their relatively coarse time resolution.

220   Taking the results of all weekly samples as a whole, atmospheric NH_3 concentrations

221   in Shanghai range from 1.2 to 23.1 ppb, with a mean (± 1σ) and median value of 7.3 (±

222   3.1) and 6.8 ppb, respectively. Domestically, the annual average NH_3 concentrations in

223   northern China (e.g., Beijing (23.5 ± 18.0 ppb)[82] and Xi'an (18.6 ppb on average)[83]) are

224   much higher than our observations in Shanghai (Table 2). This can be partly explained

225   by a higher soil pH in the North China Plain and the Guanzhong Plain where Beijing and

226   Xi'an are located, respectively,[84] which promotes loss of NH_3.[85] Instead, the Yangtze

227   River Delta region (including Shanghai) is dominated by acid soils of paddy fields.[86]

228   Internationally, the average NH_3 level we measured in Shanghai is generally similar to

229   observations in developed cities like Seoul in S. Korea[87] and Houston in the U.S.,[88] but

230   much lower than in some cities in developing countries. This is particularly true when

231   comparing with cities in South Asia (e.g., Delhi in India;[89] Table 2), where there is a lack

232   of basic sanitation facilities (e.g., public flush toilets), and significant animal populations

233   (such as cows) coexist with people in urban areas.[90] The high NH_3 concentrations

234   measured at surface sites in South Asia are consistent with the spatial patterns

235   determined from recent satellite remote sensing observations.[91, 92] It is worth noting that

236   from measurements in the Shanghai Jinshan chemical industry park (Fig. 2), Wang et

237   al.[93] showed a much higher NH_3 concentration (17.6 ± 9.5 ppb) with abrupt

238   concentration changes on an hourly basis, a result of the strong influence of variable

239   industrial emissions in the vicinity.

240   NH_3 levels were found to exhibit modest gradients across the study region, with mean

241   NH_3 concentrations ranging from 4.8 (CM rural site) to 9.7 ppb (HP urban site) (Fig. 2

242   and Fig. 3c). As discussed above, on a regional scale, NH_3 is mainly emitted from

243   animal housing, manure storage, and land-spread manure, and to a smaller extent from

244   mineral fertilizer application. The emission strengths of these sources are primarily

245   determined by the activity of microbes, which is highly dependent on temperature.[94]

246   Hence, rural areas with strong agricultural sources, are expected to experience

247   increased emissions in summertime. Indeed, in our study, the average NH_3

248   concentrations in summer are higher than in other seasons for each land use category

249   (Fig. 3b) and site (Fig. 3d), signifying the importance of volatilized NH_3 sources in the

250   region (see discussion later). Somewhat surprisingly, however, the lowest average

251   ambient NH_3 concentrations are found at rural sites such as CM (4.8 ± 2.6 ppb) and SY

252   (6.3 ± 4.1 ppb), which are in active agricultural areas (Fig. 3c). Although the average

253   NH_3 concentration at the rural DH site (7.4 ± 4.1 ppb) is higher than 7 of the other 13

254   sites (Fig. 3c), the overall average NH_3 concentration observed at urban sites (7.8 ± 2.9

255   ppb) is significantly higher than at suburban (6.8 ± 3.1 ppb, $p < 0.01$) and rural (6.2 ±

256   3.8 ppb, $p < 0.01$) sites (Fig. 3a). In fact, urban enrichment of NH_3 in Shanghai is not

257   unique. In Table 2 we compile previous studies in which urban NH_3 concentrations are

258   comparable with or higher than suburban and rural NH_3 concentrations. In brief, our

259   results demonstrate that urban areas, without agricultural activities, can also be an

260   important source of NH_3 emissions.

261   Temperature is the key driver of NH_3 emissions from volatility-driven sources;

262   observations of NH_3 volatilization by Sommer et al.[98] found that NH_3 emissions after 6 h

263   of surface applied cattle slurry were exponentially related to temperature ($r^2 > 0.80$). As

264   shown in Fig. 2 and Fig. 3d, the average NH_3 concentrations are higher in summer and

265   lower in winter. This is particularly true at rural sites, consistent with dominant,

266   temperature-sensitive emission of NH_3 from agricultural sources like livestock waste and

267   fertilizer application. There are also other temperature-sensitive sources in urban areas

268   like wastewater, household garbage, golf turf, and human excreta; the latter two are

269   often overlooked but important NH_3 sources in urban China.[44, 99] Although still

270   recognized as a luxury sport by most Chinese people, golf is increasingly popular.[44] In

271   contrast to Western industrialized countries, golf courses in China tend to operate in

272   urban areas, which are closer to the affluent consumer.[44] Also different from other

273   developed countries, human excreta in urban China is typically first stored in a three-

274   grille septic tank beneath the building.[61] After a series of anaerobic decomposition

275   processes, a substantial amount of odors (including NH_3) will be generated and emitted

276   through a ceiling duct.[61]

277   From a climate perspective, differences in temperature and other meteorological

278   parameters (e.g., precipitation, wind speed, planetary boundary layer) over the

279   Shanghai region are minor.[36] Interestingly, the lowest NH_3 concentrations at urban

280   Shanghai sites were not observed in the winter, while the NH_3 difference between

281   summer and winter is much lower at urban sites than at rural sites in our dataset (Fig.

282   3). These observations suggest that there may be some other temperature-independent

283   NH_3 sources present in urban areas.

284   **3.2 Significant influences of non-agricultural NH_3 emissions in the urban atmosphere**

285   The analysis of weekly NH_3 samples collected from our network of sites spanning

286   various land use categories indicates that the enhancement of atmospheric NH_3 at

287   urban sites reflects a mix of agricultural and non-agricultural NH_3 emissions. To further

288   explore and compare the influences of various NH_3 sources on ambient NH_3 in urban

289   and rural atmospheres, we can examine the year-round, hourly observations of NH_3 at

290   the urban PD and rural DH sites (Fig. 1). By combining hourly concentration, wind

291   speed, and wind direction measurements, bivariate polar plots (BPP) can be

292   constructed to identify source regions of near-ground pollutants like NH_3, an approach

293   that has proven to be a more suitable tool than back trajectory-based methods.[78, 80, 81]

294   As illustrated in Fig. 4a, there are large temporal variations in NH_3 concentrations at

295   the urban PD and rural DH site, with their hourly NH_3 concentrations ranging from 0.1 to

296   36.4 μg m^{-3} (mean ± 1σ = 5.9 ± 4.5 μg m^{-3}; median = 4.8 μg m^{-3}; n = 7897; 90.1% data

297   availability) and 0.1 to 33.0 µg m^{-3} (mean ± 1σ = 6.6 ± 4.1 µg m^{-3}; median = 5.9 µg m^{-3};

298   n = 8204; 93.7% data availability), respectively. The NH_3 concentration spikes at both

299   sites are concentrated in summer (June, July, and August), and their smoothed trends

300   are generally consistent with the variation of temperature. These findings suggest that

301   volatilized NH_3 emissions are a regionally important NH_3 source in Shanghai.

302   Also included in Fig. 4 are, to help further identify specific sources, the diurnal profiles

303   of NH_3 and temperature at DH and PD. At the rural DH site, diurnal variations of NH_3

304   concentrations are highly correlated with temperature (r^2 = 0.98, p < 0.01; Fig. 4b),

305   indicating the predominant role of volatilization-related NH_3 sources in rural areas. In

306   eastern China (including Shanghai), agricultural sources (livestock feeding and N-

307   fertilizer application) make up nearly 90% of the total NH_3 emissions.[22] Indeed, in Fig.

308   5a, the BPP analysis shows that high NH_3 concentrations at DH are associated with air

309   flows from the southwest and the southeast but infrequently from the northwest. This

310   can be explained by the large lake Dianshanhu in the northwest, which has negligible

311   NH_3 emission potential.[44, 45] The south and east side of the lake is covered by intensive

312   cultivation areas, with modern agriculture facilities.[61] The areas to the southeast of the

313   sampling site have been described as the "backyard garden" of Shanghai, renowned for

314   its idyllic scene, and are a regional hot spot of agricultural NH_3 emissions.[22, 61]

315   At the urban PD site, however, distinctly different pictures of the diurnal profiles of NH_3

316   and temperature are observed (see Fig. 4c and 4d), suggesting a complex mix of NH_3

317   source contributions. Specifically, there is no correlation between NH_3 concentration

318   and temperature on a diurnal basis (Fig. 4d). The average concentrations of NH_3 show

319   a well-marked bimodal pattern, which is generally similar to the diurnal evolution of

320   urban traffic flow in Shanghai.[17] Previous observations have also shown coincident

321   enhancements of NH_3 and carbon monoxide (CO) in the Shanghai urban atmosphere.[36]

322   Following a stable period of NH_3 concentrations between 22:00 and 5:00 (5.7 ± 0.1 μg

323   m^{-3}), the maximum NH_3 concentration occurs in the morning rush hour (7.0 μg m^{-3},

324   10:00), 22% higher than the overnight level. In Fig. 5b, the Shanghai metropolitan area

325   to the southwest and the suburban Pudong District to the southeast are indicated as two

326   prominent NH_3 source regions. The metropolitan area is densely populated with intense

327   traffic, representing an important source region of non-agricultural NH_3 emissions

328   (including vehicles). The suburban Pudong District, for long stretches, serves as the

329   primary animal feeding operation region in Eastern China, where almost all livestock

330   farms are focused on hog rearing.[61]

331   To further examine the NH_3 emissions potential from vehicles, we measured NH_3

332   concentrations emitted from tailpipe exhaust of 19 different vehicles equipped with

333   TWCs. The average NH_3 concentration of the total 57 samples (10.2 ppm) is four orders

334   of magnitude higher than the ambient NH_3 concentrations. Considering the huge

335   automobile inventory in Shanghai (nearly 3.3 million in 2015),[36] our study strongly

336   suggests that on-road traffic is an important NH_3 source in the urban atmosphere.

337   **3.3 NH_3 from non-agricultural rival agricultural emissions in the urban atmosphere**

338   Figure 6 compares model simulations and measurements of hourly NH_3 concentration

339   at the rural DH and urban PD sites. The average measured and predicted NH_3

340   concentrations at DH are similar, although the variability in the model predictions is

341   much larger than the observations, perhaps reflecting the coarse time resolution of the

342   emission inventory used. It is noteworthy that the average NH_3 concentration at the rural

343   DH site is accurate without any non-agricultural NH_3 emissions being included in the

344   model, consistent with our conclusion above that agricultural activities are the

345   predominant NH_3 source in rural areas. At the urban PD site, the simulation with only

346   agricultural NH_3 emissions yields an average predicted NH_3 concentration (3.6 μg m^{-3})

347   that is 47% lower than the average measured concentration (6.7 μg m^{-3}), suggesting

348   that (non-simulated) emissions from non-agricultural activities are important contributors

349   to urban NH_3. Although other factors could contribute to under-prediction of urban NH_3

350   (e.g., incorrectly modeled transport from rural agricultural sources or overestimation of

351   the rate of dry deposition of NH_3 emitted by agricultural sources), past studies suggest

352   that ambient NH_3 concentrations most strongly depend on NH_3 emissions rather than

353   atmospheric processes,[100, 101] suggesting that ignoring non-agricultural NH_3 emissions

354   is likely one of the most important reasons for the low concentration model bias at PD.

355   A quantitative and accurate assessment of NH_3 sources in the urban atmosphere is

356   difficult to obtain solely using the approach described above. Below we demonstrate the

357   complementary use of N isotopes to better constrain NH_3 source contributions at the PD

358   site. Although there is generally not a compelling need to differentiate agricultural vs.

359   non-agricultural emissions contributions in rural areas, the relative contributions of N-

360   fertilizer application and livestock feeding are certainly of interest and isotopic

361   signatures are also used to constrain these source contributions at the rural DH site.

362   Isotope-based source apportionment of atmospheric NH_3 requires a well-established

363   pool of NH_3 isotopic source signatures (δ^{15}N-NH_3) to allow a separation of different

364   sources. From a total of 44 NH_3 source samples in our previous study,[65] we have

365   established a pool of isotopic signatures for the major NH_3 emission sources in Eastern

366   China (Table 1). The NH_3 concentrations and δ^{15}N values of these samples ranged from

367   33 to 6211 μg m^{-3} and -52.0 to -9.6‰, respectively. Recently, NH_3 slip from coal-fired

368   power plants equipped with selective catalytic reduction (SCR) technology was reported

369   as an important source of NH_3; thus, its isotopic signature, as reported by Felix et al.[76],

370   is also considered in this study. Table 1 shows that these NH_3 sources can be clearly

371   classified into four categories by specific isotope signatures: NH_3 emitted from

372   combustion-related sources has relatively high δ^{15}N values, allowing them to be

373   distinguished from NH_3 emitted from volatilization processes. The δ^{15}N values (mean ±

374   1σ) of the Shanghai urban PD site environmental samples collected in July and August

375   of 2015 were -31.72 ± 3.36‰ (ranging from -36.01‰ to -25.40‰, n = 10), close to the

376   δ^{15}N-NH$_3$ values observed in Beijing (-34.0‰ to -27.2‰, n = 4; a period without strict air

377   quality control measures)[65] and higher than at the rural DH site (-41.03‰, -36.53‰),

378   suggesting a stronger influence of combustion-related sources in the urban atmosphere.

379   At the rural DH site, our earlier analysis demonstrated that rural NH$_3$ concentrations

380   can be solely attributed to agricultural NH$_3$ emissions, i.e., livestock breeding (LB) and

381   fertilizer application (FA). Therefore, the isotopic signatures of two sources, i.e., LB and

382   FA, are used as input into the SIAR Bayesian mixing model. The results suggest that on

383   average, LB and FA contribute 51.9% and 48.1% to the measured NH$_3$ concentrations,

384   respectively (not shown). From the perspective of the emissions inventory, the NH$_3$

385   emissions from LB and FA contribute 48% and 40% to the total in Eastern China,

386   respectively,[22] in general agreement with our results.

387   At the PD urban site with its more complex NH$_3$ sources, normal distributions and

388   variation ranges (within 5 and 95 percentiles) of the relative contribution fractions of

389   each source to the ambient NH$_3$ concentrations were estimated and are depicted in Fig.

390   7. As a reminder, the availability of only a single isotopic tracer vs. four hypothesized

391   source types, means that there is no unique solution for the system;[102, 103] however, we

392   can identify all possible sets of source contributions that reproduce the observed

393   isotopic signature. The utility of this analysis will depend, to a large extent, on how

394   narrow the source contribution ranges are for each source. In our analysis, fossil fuel-

395   related sources (FF) and fertilizer application (FA) have relatively low variation ranges

396   (Fig. 7), indicating that they are better constrained than livestock breeding (LB; -31.7%

397   to -27.1%) and urban waste volatilized (UW; -41.9% to -29.9%) sources. This is

398   because the isotopic signatures of LB and UW are distributed in the middle of the

399   source pool, where their contributions to the $\delta^{15}N$ values of the ambient NH_3 (-36.01‰

400   to -25.40‰) are less well constrained. The pie chart in Fig. 7 illustrates the overall mean

401   contribution proportions.. While estimates of the mean values are inherently

402   uncertain,[102] the four source contribution distribution estimates strongly suggest that all

403   four source types make substantial contributions to the NH_3 concentrations measured at

404   the urban PD site. Further, this isotopic analysis lends further confidence to our earlier

405   conclusion from the WRF-CMAQ model vs. observations comparison that non-

406   agricultural sources rival agricultural sources in terms of contributing to ambient NH_3 in

407   the urban atmosphere.

408   Fossil fuel-related sources are identified as an important contributor to ambient NH_3

409   concentrations at PD. Although NH_3 emissions from coal and biomass burning are

410   observed,[26, 30] they are not comparable with the magnitude of vehicular NH_3 emissions

411   and NH_3 slip from SCR-equipped coal-fired power plant (CFPP).[30, 37] Recently, a five-

412   year plan was introduced in China to slash coal consumption from CFPP and household

413   sectors.[77] For example, in 2016, all CFPPs in Beijing were replaced with gas-fired

414   power plants to cut pollution.[77] The replacement by the four gas-fired power plants will

415   help cut emissions by 10000 tons of SO_2 and 19000 tons of NO annually.[77] Although

416   NH_3 slip is a common issue with SCR technology used in CFPP for the removal of NO,

417   the mass concentration of NH_3 (typically 3-5 mg NH_3 m^{-3}) in flue gases is two or three

418   orders of magnitude smaller than that of NO_x.[77] Therefore, we suspect that the share of

419   NH_3 emissions from SCR-equipped CFPP in urban areas is relatively small and will

420   decrease continuously in China. In the US, it is estimated that 5% of the national NH_3

421   emissions are derived from motor vehicles, while this figure is estimated at 12% for the

422   UK, with almost all the remaining NH_3 coming from agricultural processes.[45] In China,

423   all new light-duty vehicles were required to install TWC since 2009.[44] In Table S1, we

424   have provided direct evidence that TWC-equiped vehicles are an important urban

425   source of NH_3. Thus expanding vehicular NH_3 emissions in urban China can be

426   expected. Indeed, the average contribution of fossil fuel-related sources derived from

427   the Bayesian isotopic mixing model (28.6%) is close to the share of on-road traffic

428   (22.3%) we estimated above based on NH_3 concentration analysis at PD. This suggests

429   that fossil fuel-derived NH_3 concentrations in urban Shanghai are primarily emitted from

430   on-road traffic.

431   **4 Implications and outlook**

432   The present study outlines a framework to integrate NH_3 concentration

433   measurements, atmospheric transport modeling, and isotope-based source

434   apportionment to address a long-standing and ongoing controversy regarding sources

435   of NH_3 in the urban atmosphere. We validate the feasibility of this approach by

436   application to the Yangtze River Delta region, with a focus on the megacity of Shanghai.

437   Results from a Shanghai passive NH_3 monitoring network (14 locations) reveal a

438   broadly homogeneous distribution of NH_3 concentrations throughout the region and

439   pinpoint urban areas as a hot spot of NH_3. The acquired data also provide a baseline

440   toward tracking future NH_3 emissions changes. The year-round online measurements of

441   NH_3 at an urban and rural site, and a comparison against concentrations simulated by

442   the WRF-CMAQ chemical transport model, demonstrate that NH_3 in the rural

443   atmosphere can be attributed to emissions from agricultural sources, while there is a

444   significant contribution from non-agricultural NH_3 emissions, particularly vehicular NH_3

445   emissions, in the urban atmosphere. Isotope-based source apportionment of NH_3 in the

446   urban atmosphere further indicates that non-agricultural NH_3 emissions, missing from

447   the current emission inventory, could well rival agricultural NH_3 emissions in terms of

448   contributing to ambient NH_3.

449   Given the central role of NH_3 in the formation of secondary inorganic aerosols and

450   resulting haze, our results are of critical importance for China as it seeks to curb its

451   severe $PM_{2.5}$ pollution. Additional useful investigative steps could include: (1) sensitivity

452   analyses with the WRF-CMAQ model to further diagnose the importance of non-

453   agricultural NH_3 emissions through developing a gridded non-agricultural NH_3 emissions

454   inventory with high time resolution; (2) collecting NH_3 and aerosol NH_4^+ for

455   simultaneously determining the mass concentrations and isotopic compositions at high

456   time resolution; and (3) improving the pool of isotopic source signatures of NH_3 from

457   fuel-related sources.

458   ASSOCIATED CONTENT

459   **Supporting Information**.

460   The following files are available free of charge (PDF). Figure S1. A summary of the

461   average monthly temperature and precipitation in Shanghai. Text S1. Details regarding

462   the method used to collect vehicle-emitted NH_3. Text S2. Model frame and computing

463   methods of the SIAR (Stable Isotope Analysis in R).

464   AUTHOR INFORMATION

465   **Corresponding Author**

466   *Corresponding authors: Yanlin Zhang (dryanlinzhang@outlook.com), Congrui Deng

467   (congruideng@fudan.edu.cn).

468   **Notes**

469   The authors declare that they have no conflict of interest.

478   REFERENCES

479 1. Wang, Y.; Zhang, Q. Q.; He, K.; Zhang, Q.; Chai, L., Sulfate-nitrate-ammonium aerosols over China:
480 Response to 2000-2015 emission changes of sulfur dioxide, nitrogen oxides, and ammonia. *Atmos. Chem. Phys.*
481 **2013,** *13*, (5), 2635-2652.
482 2. Walker, J. M.; Philip, S.; Martin, R. V.; Seinfeld, J. H., Simulation of nitrate, sulfate, and ammonium
483 aerosols over the United States. *Atmos. Chem. Phys.* **2012,** *12*, (22), 11213-11227.
484 3. Zhang, X. Y.; Wang, Y. Q.; Niu, T.; Zhang, X. C.; Gong, S. L.; Zhang, Y. M.; Sun, J. Y., Atmospheric
485 aerosol compositions in China: Spatial/temporal variability, chemical signature, regional haze distribution and
486 comparisons with global aerosols. *Atmos. Chem. Phys.* **2012,** *12*, (2), 779-799.
487 4. Yang, F.; Tan, J.; Zhao, Q.; Du, Z.; He, K.; Ma, Y.; Duan, F.; Chen, G.; Zhao, Q., Characteristics of $PM_{2.5}$
488 speciation in representative megacities and across China. *Atmos. Chem. Phys.* **2011,** *11*, (11), 5207-5219.
489 5. Huang, R. J.; Zhang, Y.; Bozzetti, C.; Ho, K. F.; Cao, J. J.; Han, Y.; Daellenbach, K. R.; Slowik, J. G.;
490 Platt, S. M.; Canonaco, F.; Zotter, P.; Wolf, R.; Pieber, S. M.; Bruns, E. A.; Crippa, M.; Ciarelli, G.; Piazzalunga,
491 A.; Schwikowski, M.; Abbaszade, G.; Schnelle-Kreis, J.; Zimmermann, R.; An, Z.; Szidat, S.; Baltensperger, U.; El
492 Haddad, I.; Prevot, A. S., High secondary aerosol contribution to particulate pollution during haze events in China.
493 *Nature* **2014,** *514*, (7521), 218-222.
494 6. Paulot, F.; Jacob, D. J., Hidden cost of US agricultural exports: Particulate matter from ammonia
495 emissions. *Environ. Sci. Technol.* **2014,** *48*, (2), 903-908.
496 7. Pinder, R. W.; Adams, P. J.; Pandis, S. N., Ammonia emission controls as a cost-effective strategy for
497 reducing atmospheric particulate matter in the eastern United States. *Environ. Sci. Technol.* **2007,** *41*, (2), 380-386.
498 8. Heo, J.; Adams, P. J.; Gao, H. O., Public health costs of primary $PM_{2.5}$ and inorganic $PM_{2.5}$ precursor
499 emissions in the United States. *Environ. Sci. Technol.* **2016,** *50*, (11), 6061-6070.
500 9. Brunekreef, B.; Harrison, R. M.; Künzli, N.; Querol, X.; Sutton, M. A.; Heederik, D. J. J.; Sigsgaard, T.,
501 Reducing the health effect of particles from agriculture. *Lancet Respiratory Medicine* **2015,** *3*, (11), 831-832.
502 10. Lee, C. J.; Martin, R. V.; Henze, D. K.; Brauer, M.; Cohen, A.; Donkelaar, A. V., Response of global
503 particulate-matter-related mortality to changes in local precursor emissions. *Environ. Sci. Technol.* **2015,** *49*, (7),
504 4335-4344.
505 11. Warner, J. X.; Dickerson, R. R.; Wei, Z.; Strow, L. L.; Wang, Y.; Liang, Q., Increased atmospheric
506 ammonia over the world's major agricultural areas detected from space. *Geophys. Res. Lett.* **2017,** *44*, (6), 2875-
507 2884.
508 12. Liu, L.; Zhang, X.; Xu, W.; Liu, X.; Li, Y.; Lu, X.; Zhang, Y.; Zhang, W., Temporal characteristics of
509 atmospheric ammonia and nitrogen dioxide over China based on emission data, satellite observations and
510 atmospheric transport modeling since 1980. *Atmos. Chem. Phys.* **2017,** *17*, (15), 9365-9378.
511 13. Kang, Y.; Liu, M.; Song, Y.; Huang, X.; Yao, H.; Cai, X.; Zhang, H.; Kang, L.; Liu, X.; Yan, X.; He, H.;
512 Zhang, Q.; Shao, M.; Zhu, T., High-resolution ammonia emissions inventories in China from 1980 to 2012. *Atmos.*
513 *Chem. Phys.* **2016,** *16*, (4), 2043-2058.
514 14. Aneja, V. P.; Schlesinger, W. H.; Erisman, J. W., Farming pollution. *Nat. Geosci.* **2008,** *1*, (7), 409-411.
515 15. Reis, S.; Pinder, R.; Zhang, M.; Lijie, G.; Sutton, M., Reactive nitrogen in atmospheric emission
516 inventories. *Atmos. Chem. Phys.* **2009,** *9*, (19), 7657-7677.
517 16. Van Damme, M.; Wichink Kruit, R. J.; Schaap, M.; Clarisse, L.; Clerbaux, C.; Coheur, P.; Dammers, E.;
518 Dolman, A. J.; Erisman, J. W., Evaluating 4 years of atmospheric ammonia (NH_3) over Europe using IASI satellite
519 observations and LOTOS-EUROS model results. *J. Geophys. Res.* **2014,** *119*, (15), 9549-9566.
520 17. Xu, P.; Liao, Y. J.; Lin, Y. H.; Zhao, C. X.; Yan, C. H.; Cao, M. N.; Wang, G. S.; Luan, S. J., High-
521 resolution inventory of ammonia emissions from agricultural fertilizer in China from 1978 to 2008. *Atmos. Chem.*
522 *Phys.* **2016,** *16*, (3), 1207-1218.
523 18. Bouwman, A. F.; Lee, D. S.; Asman, W. A. H.; Dentener, F. J.; Van Der Hoek, K. W.; Olivier, J. G. J., A
524 global high-resolution emission inventory for ammonia. *Global Biogeochem. Cy.* **1997,** *11*, (4), 561-587.
525 19. Heald, C. L.; Collett Jr, J.; Lee, T.; Benedict, K.; Schwandner, F.; Li, Y.; Clarisse, L.; Hurtmans, D.; Van
526 Damme, M.; Clerbaux, C., Atmospheric ammonia and particulate inorganic nitrogen over the United States. *Atmos.*
527 *Chem. Phys.* **2012,** *12*, (21), 10295-10312.
528 20. Zhang, L.; Chen, Y.; Zhao, Y.; Henze, D. K.; Zhu, L.; Song, Y.; Paulot, F.; Liu, X.; Pan, Y.; Lin, Y.;
529 Huang, B., Agricultural ammonia emissions in China: Reconciling bottom-up and top-down estimates. *Atmos.*
530 *Chem. Phys.* **2018,** *18*, (1), 339-355.

531	21.	Balasubramanian, S.; Koloutsou-Vakakis, S.; McFarland, D. M.; Rood, M. J., Reconsidering emissions of
532	ammonia from chemical fertilizer usage in Midwest USA. *J. Geophys. Res.* **2015,** *120*, (12), 6232-6246.
533	22.	Huang, C.; Chen, C. H.; Li, L.; Cheng, Z.; Wang, H. L.; Huang, H. Y.; Streets, D. G.; Wang, Y. J.; Zhang,
534	G. F.; Chen, Y. R., Emission inventory of anthropogenic air pollutants and VOC species in the Yangtze River Delta
535	region, China. *Atmos. Chem. Phys.* **2011,** *11*, (9), 4105-4120.
536	23.	Aneja, V. P.; Schlesinger, W. H.; Erisman, J. W., Effects of agriculture upon the air quality and climate:
537	Research, policy, and regulations. *Environ. Sci. Technol.* **2009,** *43*, (12), 4234-4240.
538	24.	Wang, S.; Xing, J.; Jang, C.; Zhu, Y.; Fu, J. S.; Hao, J., Impact assessment of ammonia emissions on
539	inorganic aerosols in East China using response surface modeling technique. *Environ. Sci. Technol.* **2011,** *45*, (21),
540	9293-300.
541	25.	Zhang, C.; Geng, X.; Wang, H.; Zhou, L.; Wang, B., Emission factor for atmospheric ammonia from a
542	typical municipal wastewater treatment plant in South China. *Environ. Pollut.* **2017,** *220*, 963-970.
543	26.	Li, Q.; Jiang, J.; Cai, S.; Zhou, W.; Wang, S.; Duan, L.; Hao, J., Gaseous ammonia emissions from coal and
544	biomass combustion in household stoves with different combustion efficiencies. *Environ. Sci. Technol. Lett.* **2016,** *3*,
545	(3), 98-103.
546	27.	Reche, C.; Viana, M.; Pandolfi, M.; Alastuey, A.; Moreno, T.; Amato, F.; Ripoll, A.; Querol, X., Urban
547	NH$_3$ levels and sources in a Mediterranean environment. *Atmos. Environ.* **2012,** *57*, 153-164.
548	28.	Suarez-Bertoa, R.; Zardini, A.; Astorga, C., Ammonia exhaust emissions from spark ignition vehicles over
549	the new European driving cycle. *Atmos. Environ.* **2014,** *97*, 43-53.
550	29.	Teng, X.; Hu, Q.; Zhang, L.; Qi, J.; Shi, J.; Xie, H.; Gao, H.; Yao, X., Identification of major sources of
551	atmospheric NH$_3$ in an urban environment in Northern China during wintertime. *Environ. Sci. Technol.* **2017,** *51*,
552	(12), 6839-6848.
553	30.	Meng, W.; Zhong, Q.; Yun, X.; Zhu, X.; Huang, T.; Shen, H.; Chen, Y.; Chen, H.; Zhou, F.; Liu, J.; Wang,
554	X.; Zeng, E. Y.; Tao, S., Improvement of a global high-resolution ammonia emission inventory for combustion and
555	industrial sources with new data from the residential and transportation sectors. *Environ. Sci. Technol.*, **2017**, *51* (5),
556	2821-2829.
557	31.	Pierson, W. R.; Brachaczek, W. W., Emissions of ammonia and amines from vehicles on the road. *Environ.*
558	*Sci. Technol.* **1983,** *17*, (12), 757-760.
559	32.	Heeb, N. V.; Forss, A. M.; Brühlmann, S.; Lüscher, R.; Saxer, C. J.; Hug, P., Three-way catalyst-induced
560	formation of ammonia—velocity-and acceleration-dependent emission factors. *Atmos. Environ.* **2006,** *40*, (31),
561	5986-5997.
562	33.	Fenn, M. E.; Bytnerowicz, A.; Schilling, S. L.; Vallano, D. M.; Zavaleta, E. S.; Weiss, S. B.; Morozumi,
563	C.; Geiser, L. H.; Hanks, K., On-road emissions of ammonia: an underappreciated source of atmospheric nitrogen
564	deposition. *Sci. Total Environ.* **2018,** *625*, 909-919.
565	34.	Kean, A. J.; Harley, R. A.; Littlejohn, D.; Kendall, G. R., On-road measurement of ammonia and other
566	motor vehicle exhaust emissions. *Environ. Sci. Technol.* **2000,** *34*, (17), 3535-3539.
567	35.	Zhang, Y.; Tang, A.; Wang, D.; Wang, Q.; Benedict, K.; Zhang, L.; Liu, D.; Li, Y.; Collett Jr., J. L.; Sun,
568	Y.; Liu, X., The vertical variability of ammonia in urban Beijing, China. *Atmos. Chem. Phys.* **2018,** *18*, 16385-
569	16398.
570	36.	Chang, Y.; Zou, Z.; Deng, C.; Huang, K.; Collett, J. L.; Lin, J.; Zhuang, G., The importance of vehicle
571	emissions as a source of atmospheric ammonia in the megacity of Shanghai. *Atmos. Chem. Phys.* **2016,** *16*, (5),
572	3577-3594.
573	37.	Sun, K.; Tao, L.; Miller, D. J.; Pan, D.; Golston, L. M.; Zondlo, M. A.; Griffin, R. J.; Wallace, H. W.;
574	Leong, Y. J.; Yang, M. M.; Zhang, Y.; Mauzerall, D. L.; Zhu, T., Vehicle emissions as an important urban ammonia
575	source in the United States and China. *Environ. Sci. Technol.* **2017,** *51*, (4), 2472-2481.
576	38.	Fraser, M. P.; Cass, G. R., Detection of excess ammonia emissions from in-use vehicles and the
577	implications for fine particle control. *Environ. Sci. Technol.* **1998,** *32*, (8), 1053-1057.
578	39.	Huai, T.; Durbin, T. D.; Miller, J. W.; Pisano, J. T.; Sauer, C. G.; Rhee, S. H.; Norbeck, J. M., Investigation
579	of NH$_3$ emissions from new technology vehicles as a function of vehicle operating conditions. *Environ. Sci.*
580	*Technol.* **2003,** *37*, (21), 4841-4847.
581	40.	Liu, T.; Wang, X.; Wang, B.; Ding, X.; Deng, W.; Lü, S.; Zhang, Y., Emission factor of ammonia (NH$_3$)
582	from on-road vehicles in China: Tunnel tests in urban Guangzhou. *Environ. Res. Lett.* **2014,** *9*, (6), 064027.

583   41.   Kean, A. J.; Littlejohn, D.; Ban-Weiss, G. A.; Harley, R. A.; Kirchstetter, T. W.; Lunden, M. M., Trends in
584   on-road vehicle emissions of ammonia. *Atmos. Environ.* **2009**, *43*, (8), 1565-1570.
585   42.   Nowak, J. B.; Huey, L. G.; Russell, A. G.; Tian, D.; Neuman, J. A.; Orsini, D.; Sjostedt, S. J.; Sullivan, A.
586   P.; Tanner, D. J.; Weber, R. J.; Nenes, A.; Edgerton, E.; Fehsenfeld, F. C., Analysis of urban gas phase ammonia
587   measurements from the 2002 Atlanta Aerosol Nucleation and Real-Time Characterization Experiment (ANARChE).
588   *J. Geophys. Res.* **2006**, *111*, (D17), https://doi.org/10.1029/2006JD007113.
589   43.   Yao, X.; Hu, Q.; Zhang, L.; Evans, G. J.; Godri, K. J.; Ng, A. C., Is vehicular emission a significant
590   contributor to ammonia in the urban atmosphere? *Atmos. Environ.* **2013**, *80*, 499-506.
591   44.   Chang, Y. H., Non-agricultural ammonia emissions in urban China. *Atmos. Chem. Phys. Discussions* **2014,**
592   *14*, (6), 8495-8531.
593   45.   Sutton, M. A.; Dragosits, U.; Tang, Y.; Fowler, D., Ammonia emissions from non-agricultural sources in
594   the UK. *Atmos. Environ.* **2000**, *34*, (6), 855-869.
595   46.   Battye, W.; Aneja, V. P.; Roelle, P. A., Evaluation and improvement of ammonia emissions inventories.
596   *Atmos. Environ.* **2003**, *37*, (27), 3873-3883.
597   47.   Li, Y.; Thompson, T. M.; Van Damme, M.; Chen, X.; Benedict, K. B.; Shao, Y.; Day, D.; Boris, A.;
598   Sullivan, A. P.; Ham, J.; Whitburn, S.; Clarisse, L.; Coheur, P. F.; Collett Jr, J. L., Temporal and spatial variability
599   of ammonia in urban and agricultural regions of northern Colorado, United States. *Atmos. Chem. Phys.* **2017**, *17*,
600   (10), 6197-6213.
601   48.   Puchalski, M. A.; Sather, M. E.; Walker, J. T.; Lehmann, C. M.; Gay, D. A.; Mathew, J.; Robarge, W. P.,
602   Passive ammonia monitoring in the United States: Comparing three different sampling devices. *J. Environ. Monit.*
603   **2011,** *13*, (11), 3156-67.
604   49.   Li, Y.; Schichtel, B. A.; Walker, J. T.; Schwede, D. B.; Chen, X.; Lehmann, C. M. B.; Puchalski, M. A.;
605   Gay, D. A.; Collett, J. L., Increasing importance of deposition of reduced nitrogen in the United States. *Proc. Natl.*
606   *Acad. Sci. U. S. A.* **2016**, *113*, (21), 5874-5879.
607   50.   Liu, X.; Zhang, Y.; Han, W.; Tang, A.; Shen, J.; Cui, Z.; Vitousek, P.; Erisman, J. W.; Goulding, K.;
608   Christie, P.; Fangmeier, A.; Zhang, F., Enhanced nitrogen deposition over China. *Nature* **2013**, *494*, 459-463.
609   51.   Lu, C.; Tian, H., Half-century nitrogen deposition increase across China: a gridded time-series data set for
610   regional environmental assessments. *Atmos. Environ.* **2014**, *97*, 68-74.
611   52.   Lü, C.; Tian, H., Spatial and temporal patterns of nitrogen deposition in China: Synthesis of observational
612   data. *J. Geophys. Res.* **2007,** *112*, (D22), https://doi.org/10.1029/2006JD007990.
613   53.   Jia, Y.; Yu, G.; He, N.; Zhan, X.; Fang, H.; Sheng, W.; Zuo, Y.; Zhang, D.; Wang, Q., Spatial and decadal
614   variations in inorganic nitrogen wet deposition in China induced by human activity. *Sci. Rep.*, **2014,** *4*, 3763.
615   54.   Liu, J.; Kuang, W.; Zhang, Z.; Xu, X.; Qing, Y.; Ning, J.; Zhou, W.; Zhang, S.; Li, R., Spatiotemporal
616   characteristics, patterns, and causes of land-use changes in China since the late 1980s. *J. Geogr. Sci.* **2014**, *24*, (2),
617   195-210.
618   55.   Ma, T.; Zhou, C.; Pei, T.; Haynie, S.; Fan, J., Quantitative estimation of urbanization dynamics using time
619   series of DMSP/OLS nighttime light data: a comparative case study from China's cities. *Remote Sens. Environ.*
620   **2012,** *124*, 99-107.
621   56.   Guan, X.; Wei, H.; Lu, S.; Dai, Q.; Su, H., Assessment on the urbanization strategy in China:
622   Achievements, challenges and reflections. *Habitat Int.* **2018,** *71*, 97-109.
623   57.   Haas, J.; Ban, Y., Urban growth and environmental impacts in Jing-Jin-Ji, the Yangtze, River Delta and the
624   Pearl River Delta. *Int. J. Appl. Earth Obs. Geoinfor.* **2014**, *30*, 42-55.
625   58.   Dahiya, B., Cities in Asia, 2012: Demographics, economics, poverty, environment and governance. *Cities*
626   **2012,** *29*, S44-S61.
627   59.   Wang, T.; Xue, L.; Brimblecombe, P.; Lam, Y. F.; Li, L.; Zhang, L., Ozone pollution in China: a review of
628   concentrations, meteorological influences, chemical precursors, and effects. *Sci. Total Environ.* **2017**, *575*, 1582-
629   1596.
630   60.   Han, L.; Zhou, W.; Li, W.; Li, L., Impact of urbanization level on urban air quality: a case of fine particles
631   (PM$_{2.5}$) in Chinese cities. *Environ. Pollut.* **2014**, *194*, 163-170.
632   61.   Chang, Y.; Deng, C.; Dore, A. J.; Zhuang, G., Human excreta as a stable and important source of
633   atmospheric ammonia in the megacity of Shanghai. *Plos One* **2015**, *10*, (12), e0144661.

634   62.   Rumsey, I.; Cowen, K.; Walker, J.; Kelly, T.; Hanft, E.; Mishoe, K.; Rogers, C.; Proost, R.; Beachley, G.;
635   Lear, G., An assessment of the performance of the Monitor for AeRosols and GAses in ambient air (MARGA): a
636   semi-continuous method for soluble compounds. *Atmos. Chem. Phys.* **2014,** *14*, (11), 5639-5658.
637   63.   Walters, W. W.; Goodwin, S. R.; Michalski, G., Nitrogen stable isotope composition (δ^{15}N) of vehicle-
638   emitted NO_x. *Environ. Sci. Technol.* **2015,** *49*, (4), 2278-2285.
639   64.   Liu, D.; Fang, Y.; Tu, Y.; Pan, Y., Chemical method for nitrogen isotopic analysis of ammonium at natural
640   abundance. *Anal. Chem.* **2014,** *86*, (8), 3787-92.
641   65.   Chang, Y.; Liu, X.; Deng, C.; Dore, A. J.; Zhuang, G., Source apportionment of atmospheric ammonia
642   before, during, and after the 2014 APEC summit in Beijing using stable nitrogen isotope signatures. *Atmos. Chem.*
643   *Phys.* **2016,** *16*, (18), 11635-11647.
644   66.   Hu, J.; Chen, J.; Ying, Q.; Zhang, H., One-year simulation of ozone and particulate matter in China using
645   WRF/CMAQ modeling system. *Atmos. Chem. Phys.* **2016,** *16*, (16), 10333-10350.
646   67.   Layman, C. A.; Araujo, M. S.; Boucek, R.; Hammerschlag-Peyer, C. M.; Harrison, E.; Jud, Z. R.; Matich,
647   P.; Rosenblatt, A. E.; Vaudo, J. J.; Yeager, L. A.; Post, D. M.; Bearhop, S., Applying stable isotopes to examine
648   food-web structure: an overview of analytical tools. *Biological Reviews* **2012,** *87*, (3), 545-562.
649   68.   Ward, E. J.; Semmens, B. X.; Phillips, D. L.; Moore, J. W.; Bouwes, N., A quantitative approach to
650   combine sources in stable isotope mixing models. *Ecosphere* **2011,** *2*, (2), 19.
651   69.   Zong, Z.; Wang, X.; Tian, C.; Chen, Y.; Fang, Y.; Zhang, F.; Li, C.; Sun, J.; Li, J.; Zhang, G., First
652   Assessment of NO_x sources at a regional background site in North China using isotopic analysis linked with
653   modeling. *Environ. Sci. Technol.* **2017,** *51*, (11), 5923-5931.
654   70.   Parnell, A. C.; Inger, R.; Bearhop, S.; Jackson, A. L., Source partitioning using stable isotopes: coping with
655   too much variation. *Plos One* **2010,** *5*, (3), e9672.
656   71.   Ward, E. J.; Semmens, B. X.; Schindler, D. E., Including source uncertainty and prior information in the
657   analysis of stable isotope mixing models. *Environ. Sci. Technol.* **2010,** *44*, (12), 4645-4650.
658   72.   Divers, M. T.; Elliott, E. M.; Bain, D. J., Quantification of nitrate sources to an urban stream using dual
659   nitrate isotopes. *Environ. Sci. Technol.* **2014,** *48*, (18), 10580-10587.
660   73.   Blumenthal, S. A.; Chritz, K. L.; Rothman, J. M.; Cerling, T. E., Detecting intraannual dietary variability in
661   wild mountain gorillas by stable isotope analysis of feces. *Proc. Natl. Acad. Sci. U. S. A.* **2012,** *109*, (52), 21277-
662   21282.
663   74.   Rutz, C.; Bluff, L. A.; Reed, N.; Troscianko, J.; Newton, J.; Inger, R.; Kacelnik, A.; Bearhop, S., The
664   ecological significance of tool use in new Caledonian crows. *Science* **2010,** *329*, (5998), 1523-1526.
665   75.   Palacio, S.; Azorín, J.; Montserrat-Martí, G.; Ferrio, J. P., The crystallization water of gypsum rocks is a
666   relevant water source for plants. *Nat. Commun.* **2014,** *5*, 4660.
667   76.   Felix, J. D.; Elliott, E. M.; Gish, T. J.; McConnell, L. L.; Shaw, S. L., Characterizing the isotopic
668   composition of atmospheric ammonia emission sources using passive samplers and a combined oxidation-bacterial
669   denitrifier approach. *Rapid Commun. Mass Sp.* **2013,** *27*, (20), 2239-2246.
670   77.   Chang, Y.; Ma, H., Comment on "Fossil fuel combustion-related emissions dominate atmospheric
671   ammonia sources during severe haze episodes: Evidence from ^{15}N-stable isotope in size-resolved aerosol
672   ammonium". *Environ. Sci. Technol.* **2016,** *50*, (19), 10765-10766.
673   78.   Carslaw, D. C.; Beevers, S. D.; Ropkins, K.; Bell, M. C., Detecting and quantifying aircraft and other on-
674   airport contributions to ambient nitrogen oxides in the vicinity of a large international airport. *Atmos. Environ.* **2006,**
675   *40*, (28), 5424-5434.
676   79.   Carslaw, D. C.; Ropkins, K., Openair — An R package for air quality data analysis. *Environ. Modell.*
677   *Softw.* **2012,** *27*, 52-61.
678   80.   Chang, Y.; Deng, C.; Cao, F.; Cao, C.; Zou, Z.; Liu, S.; Lee, X.; Li, J.; Zhang, G.; Zhang, Y., Assessment
679   of carbonaceous aerosols in Shanghai, China – Part 1: long-term evolution, seasonal variations, and meteorological
680   effects. *Atmos. Chem. Phys.*, **2017,** *17*, 9945-9964.
681   81.   Chang, Y.; Huang, K.; Xie, M.; Deng, C.; Zou, Z.; Liu, S.; Zhang, Y., First long-term and near real-time
682   measurement of trace elements in China's urban atmosphere: temporal variability, source apportionment and
683   precipitation effect. *Atmos. Chem. Phys.*, **2018**, *18*, 11793-11812.
684   82.   Meng, Z. Y.; Lin, W. L.; Jiang, X. M.; Yan, P.; Wang, Y.; Zhang, Y. M.; Jia, X. F.; Yu, X. L.,
685   Characteristics of atmospheric ammonia over Beijing, China. *Atmos. Chem. Phys.* **2011,** *11*, (12), 6139-6151.

686   83.   Cao, J. J.; Zhang, T.; Chow, J. C.; Watson, J. G.; Wu, F.; Li, H., Characterization of Atmospheric
687   Ammonia over Xi'an, China. *Aerosol Air Qual. Res.* **2009,** *9*, (2), 277-289.
688   84.   Ju, X. T.; Xing, G. X.; Chen, X. P.; Zhang, S. L.; Zhang, L. J.; Liu, X. J.; Cui, Z. L.; Yin, B.; Christie, P.;
689   Zhu, Z. L.; Zhang, F. S., Reducing environmental risk by improving N management in intensive Chinese
690   agricultural systems. *Proc. Natl. Acad. Sci. U. S. A.* **2009,** *106*, (9), 3041-3046.
691   85.   Wei, S.; Dai, Y.; Liu, B.; Zhu, A.; Duan, Q.; Wu, L.; Ji, D.; Ye, A.; Yuan, H.; Zhang, Q.; Chen, D.; Chen,
692   M.; Chu, J.; Dou, Y.; Guo, J.; Li, H.; Li, J.; Liang, L.; Liang, X.; Liu, H.; Liu, S.; Miao, C.; Zhang, Y., A China data
693   set of soil properties for land surface modeling. *J. Adv. Model. Earth Sy.* **2013,** *5*, (2), 212-224.
694   86.   Zhao, X.; Xie, Y. X.; Xiong, Z. Q.; Yan, X. Y.; Xing, G. X.; Zhu, Z. L., Nitrogen fate and environmental
695   consequence in paddy soil under rice-wheat rotation in the Taihu lake region, China. *Plant Soil* **2009,** *319*, (1), 225-
696   234.
697   87.   Kang, C. M.; Lee, H. S.; Kang, B. W.; Lee, S. K.; Sunwoo, Y., Chemical characteristics of acidic gas
698   pollutants and $PM_{2.5}$ species during hazy episodes in Seoul, South Korea. *Atmos. Environ.* **2004,** *38*, (28), 4749-
699   4760.
700   88.   Gong, L.; Lewicki, R.; Griffin, R. J.; Flynn, J. H.; Lefer, B. L.; Tittel, F. K., Atmospheric ammonia
701   measurements in Houston, TX using an external-cavity quantum cascade laser-based sensor. *Atmos. Chem. Phys.*
702   **2011,** *11*, (18), 9721-9733.
703   89.   Singh, S.; Kulshrestha, U. C., Abundance and distribution of gaseous ammonia and particulate ammonium
704   at Delhi, India. *Biogeosci.* **2012,** *9*, (12), 5023-5029.
705   90.   Singh, S.; Kulshrestha, U. C., Rural versus urban gaseous inorganic reactive nitrogen in the Indo-Gangetic
706   plains (IGP) of India. *Environ. Res. Lett.* **2014,** *9*, (12), 125004.
707   91.   Van Damme, M.; Clarisse, L.; Heald, C. L.; Hurtmans, D.; Ngadi, Y.; Clerbaux, C.; Dolman, A. J.;
708   Erisman, J. W.; Coheur, P. F., Global distributions, time series and error characterization of atmospheric ammonia
709   (NH_3) from IASI satellite observations. *Atmos. Chem. Phys.* **2014,** *14*, (6), 2905-2922.
710   92.   Clarisse, L.; Clerbaux, C.; Dentener, F.; Hurtmans, D.; Coheur, P. F., Global ammonia distribution derived
711   from infrared satellite observations. *Nat. Geosci.* **2009,** *2*, (7), 479-483.
712   93.   Wang, S.; Nan, J.; Shi, C.; Fu, Q.; Gao, S.; Wang, D.; Cui, H.; Saiz-Lopez, A.; Zhou, B., Atmospheric
713   ammonia and its impacts on regional air quality over the megacity of Shanghai, China. *Sci. Rep.* **2015,** *5*, (1), 15842.
714   94.   Dewes, T., Effect of pH, temperature, amount of litter and storage density on ammonia emissions from
715   stable manure. *J. Agri. Sci.* **2009,** *127*, (4), 501-509.
716   95.   Tanner, P. A., Vehicle-related ammonia emissions in Hong Kong. *Environ. Chem. Lett.* **2009,** *7*, (1), 37-40.
717   96.   Perrino, C.; Catrambone, M.; Di Bucchianico, A. D. M.; Allegrini, I., Gaseous ammonia in the urban area
718   of Rome, Italy and its relationship with traffic emissions. *Atmos. Environ.* **2002,** *36*, (34), 5385-5394.
719   97.   Hu, Q.; Zhang, L.; Evans, G. J.; Yao, X., Variability of atmospheric ammonia related to potential emission
720   sources in downtown Toronto, Canada. *Atmos. Environ.* **2014,** *99*, 365-373.
721   98.   Sommer, S. G.; Olesen, J. E.; Christensen, B. T., Effects of temperature, wind speed and air humidity on
722   ammonia volatilization from surface applied cattle slurry. *J. Agri. Sci.* **2009,** *117*, (1), 91-100.
723   99.   Cheng, H.; Hu, Y.; Reinhard, M., Environmental and Health Impacts of Artificial Turf: A Review. *Environ.*
724   *Sci. Technol.* **2014,** *48*, (4), 2114-2129.
725   100.   Asman, W. A.; Sutton, M. A.; Schjørring, J. K., Ammonia: Emission, atmospheric transport and deposition.
726   *New Phytol.* **1998,** *139*, (1), 27-48.
727   101.   Behera, S. N.; Sharma, M.; Aneja, V. P.; Balasubramanian, R., Ammonia in the atmosphere: a review on
728   emission sources, atmospheric chemistry and deposition on terrestrial bodies. *Environ. Sci. Pullut. Res. Int.* **2013,**
729   *20*, (11), 8092-8131.
730   102.   Phillips, D. L.; Gregg, J. W., Source partitioning using stable isotopes: coping with too many sources.
731   *Oecologia* **2003,** *136*, (2), 261-269.
732   103.   Chang, Y.; Zhang, Y.; Tian, C.; Zhang, S.; Ma, X.; Cao, F.; Liu, X.; Zhang, W.; Kuhn, T.; Lehmann, M. F.,
733   Nitrogen isotope fractionation during gas-to-particle conversion of NO_x to NO_3^- in the atmosphere – implications for
734   isotope-based NO_x source apportionment. *Atmos. Chem. Phys.* **2018,** *18*, (16), 11647-11661.

735
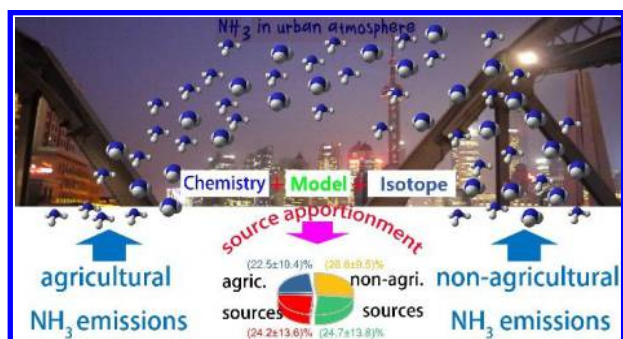
736

737   TOC art figure (8 cm*4.24 cm)
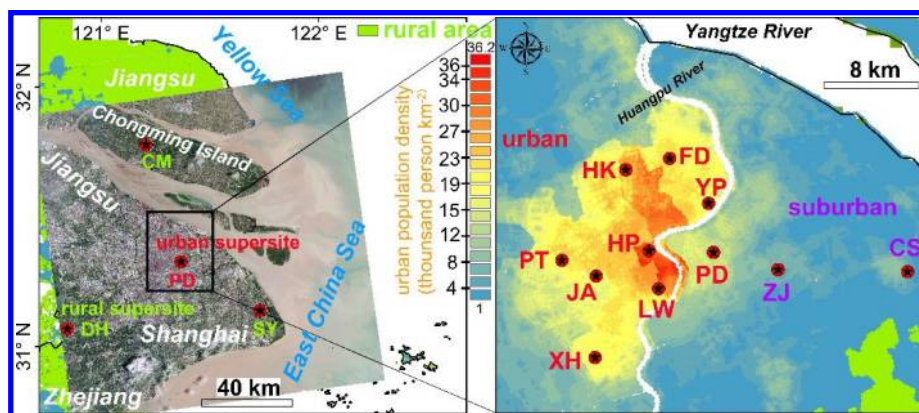
738

739

740

741

742

743

744

745

746

747   **Figure 1.** Shanghai passive ammonia monitoring network. The natural-

748   color satellite image in the left panel shows the urban area of Shanghai in 2016, along

749   with its major island Chongming. The right panel presents the population density in

750   Shanghai, which was retrieved from a newly released high-resolution (100 m × 100 m

751   per pixel) population map of China in 2010 (worldpop.org.uk).

752

753

754

755

756
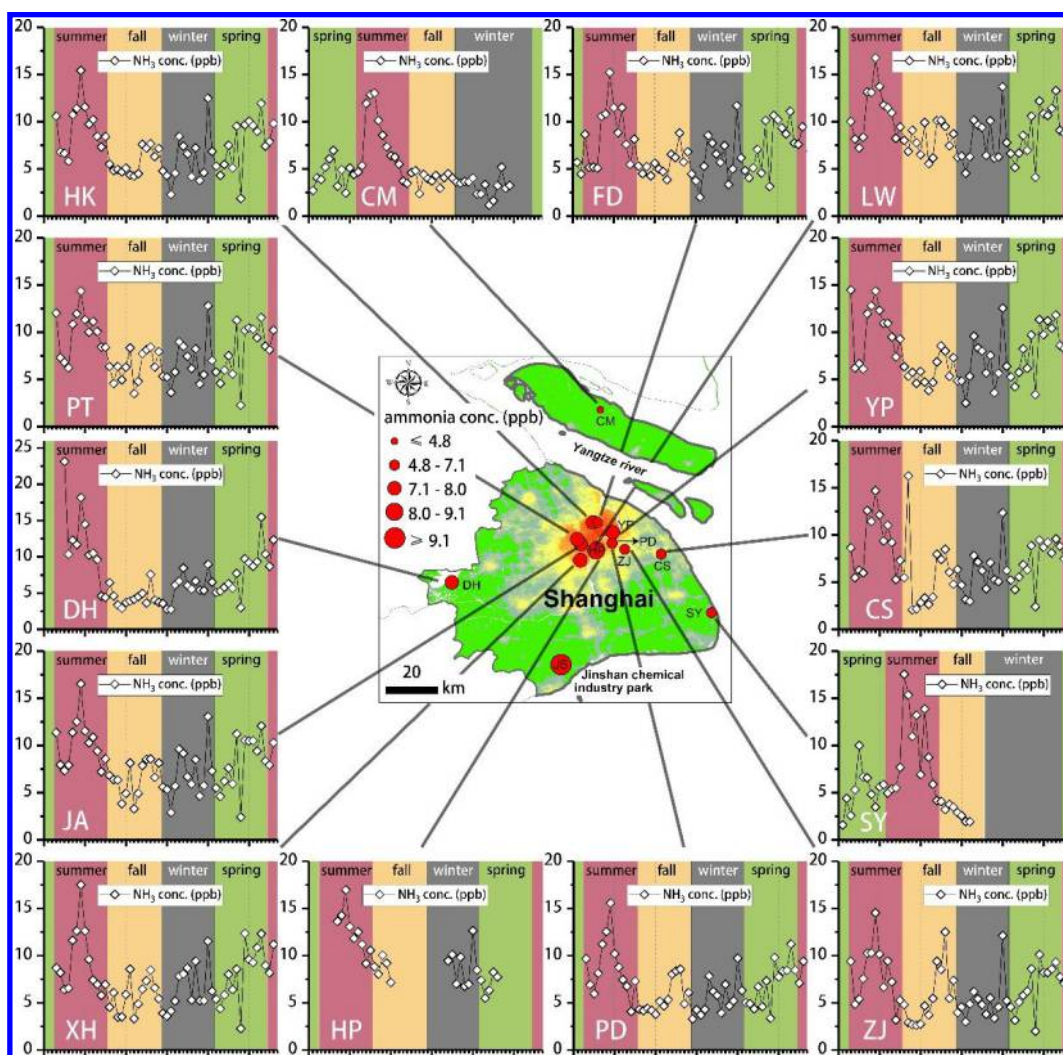
757

758   **Figure 2.** Sample-specific and group-averaged mixing ratios of ambient NH₃

759   measured with Ogawa passive samplers at fourteen surface locations in Shanghai.

760   Excepting the green color in the map (indicating rural areas), the color scheme is

761   population density with the scale the same as that in Fig. 1 (retrieved from

762   worldpop.org.uk).

763

764

765
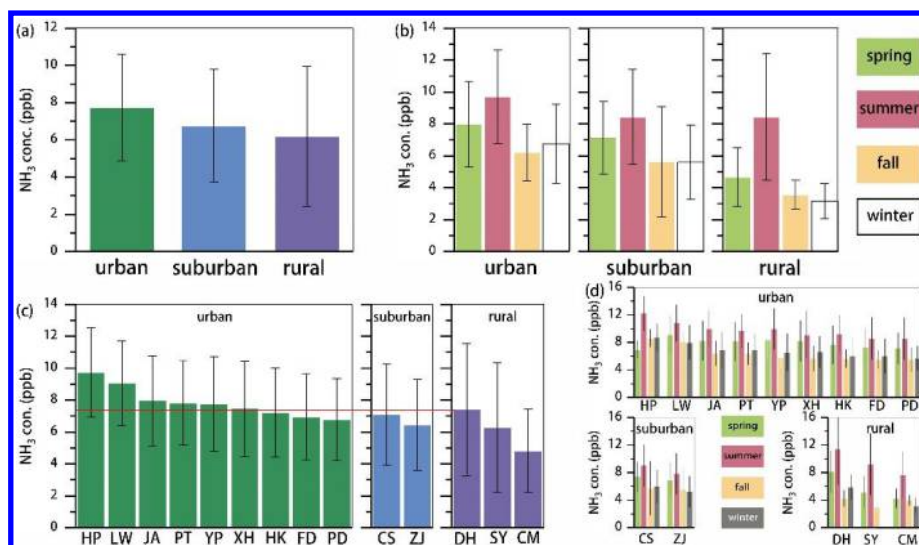
766

767   **Figure 3.** Comparison of the ambient NH$_3$ concentrations (mean ± 1σ) among (**a**)

768   different site types (urban/suburban/rural), (**b**) different seasons

769   (spring/summer/fall/winter) within a specific site type, (**c**) different individual sites, and

770   (**d**) different seasons (spring/summer/fall/winter) within a specific site.
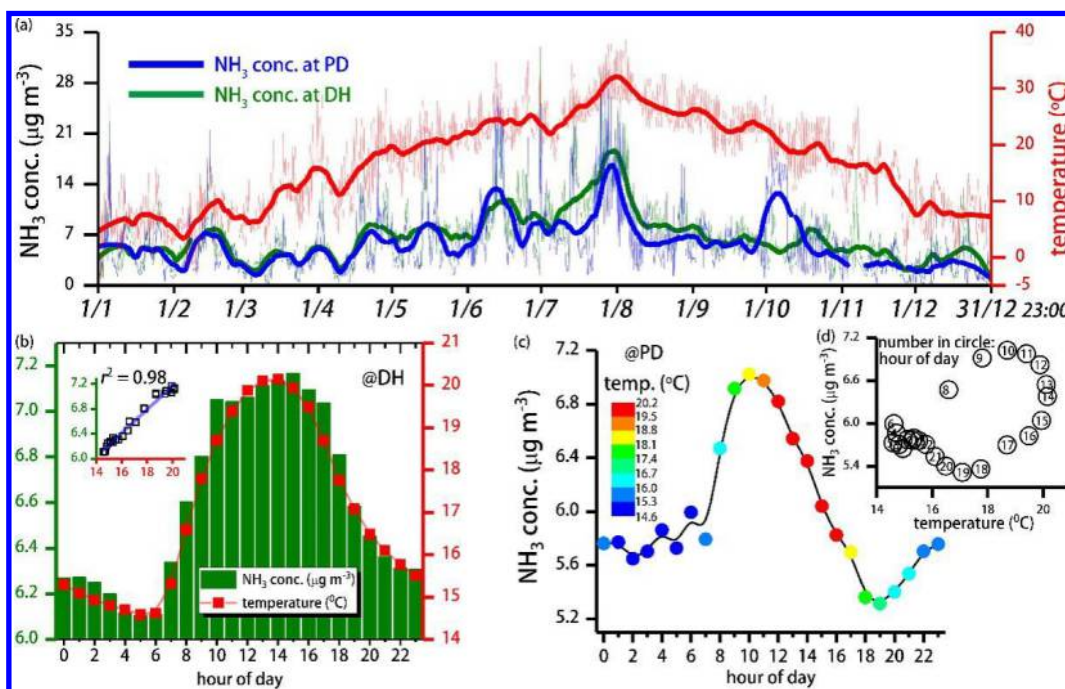
771

772

773

774

775

776

777

778

779

780   **Figure 4.** (**a**) Hourly variations of temperature (red) in Shanghai and NH_3

781   concentrations at the PD urban site (blue) and DH rural site (green), along with 500-

782   point Savitzky-Golay smoothed records from 1 January to 31 December 2015. (**b**)

783   Diurnal variation of NH_3 concentration and temperature and their correlation at DH rural

784   site in 2015. (**c**) Diurnal variation of NH_3 concentration (colored by temperature) at the

785   urban PD site in 2015. (**d**) Scatter plot of diurnal temperature and NH_3 concentration at
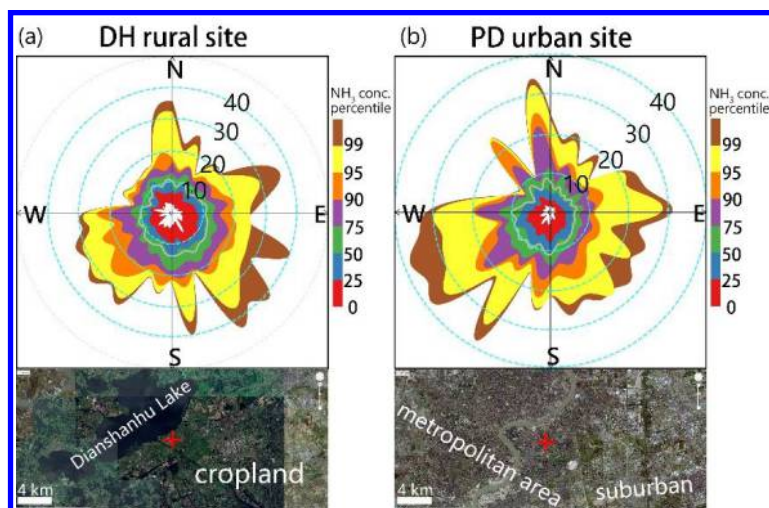
786   the urban PD site in 2015.

787

788

789

790

791

792

793   **Figure 5.** Bivariate polar plots (BPP) of the percentiles of NH_3 concentrations at (**a**)

794   rural DH site and (**b**) urban PD site. The natural-color satellite images below are the

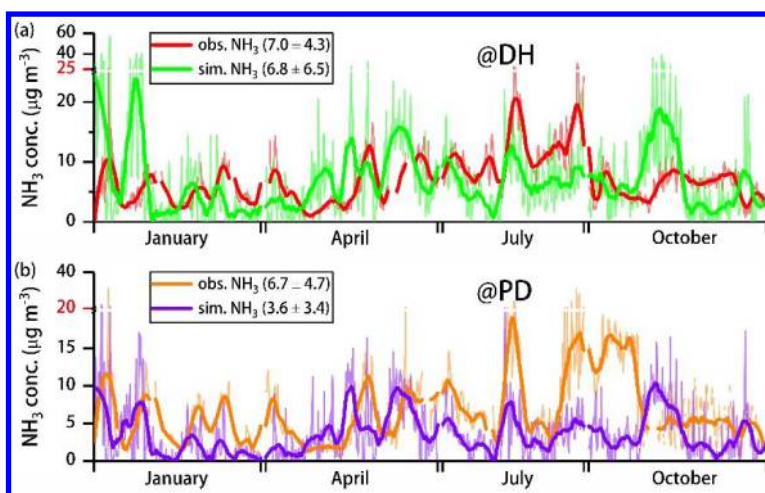795   land use maps corresponding to each site.

796

797

798

799

800

801

802

803

804

805

Figure 6. Comparison of hourly observed and simulated NH_3 concentrations at (a) DH

rural site and (b) PD urban site.
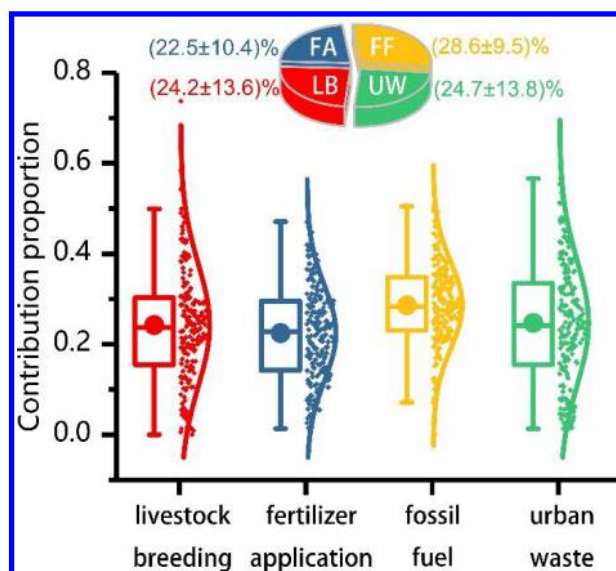
808

809

810

811

812

813

814

815

816

817

818

819   **Figure 7.** Isotope-based source apportionment of atmospheric NH_3 at PD urban site

820   with the normal distribution and variation range (within 5 and 95 percentiles).

821

822

823

824

825

826

827

828

829

830   **Table 1**. Mass concentrations and isotopic signatures ($\delta^{15}N$) of major NH_3 sources.

Category	sub-category	NH$_3$ (µg m^{-3})	δ^{15}N-NH$_3$ (‰)	N	reference
livestock breeding (LB)	pig breeding	462.2 to 1502.8	-31.7 to -27.1	7	[65]
N-fertilizer application (FA)	urea	165.6 to 623.7	-52.0 to -47.6	5	[65]
urban waste (UW)	solid waste	271.2 to 542.4	-37.6 to -29.9	8	[65]
	wastewater	127.2 to 258.5	-41.9 to -39.2	8	[65]
	human excreta	3238.0 to 6211.0	-39.6 to -37.3	8	[61]
fossil fuel-related (FF)	vehicle (road tunnel)	33.2 to 87.4	-17.8 to -9.6	8	[65]
	power plant (NH$_3$ slip)	not available	-14.6, -11.3	2	[76]

831

832

833

834

835

836

837

838

839

840

841

842

843

844

845

846

847

848   **Table 2.** Comparison of atmospheric NH_3 concentrations (in ppb) between urban and

849   suburban/rural areas in different regions.

location	period	average NH_3 concentration		reference
		urban	suburban/rural	
Shanghai, CN	2014.5-2015.6	7.8	6.8/6.2	this study
Xi'an, CN	2006.4-2007.4	18.6	20.3	[83]
Beijing, CN	2007.1-2010.7	22.8	10.2	[82]
Hong Kong, CN	2003.10-2006.5	10.2	0.2	[95]
Delhi, IN	2012.10-2013.9	52.8	65.6	[90]
Rome, IT	2001.5-2002.3	5.3	3.5	[96]
Toronto, CA	2003.7-2011.9	2.3-3.0	0.1-4	[97]

850
851

852

853